Amylose dimerization in solution can be studied using a model system

Dansholm, Charlotte Nybro; Meier, Sebastian; Beeren, Sophie R.

Published in:
ChemBioChem

Link to article, DOI:
10.1002/cbic.202300832

Publication date:
2024

Document Version
Publisher's PDF, also known as Version of record

ChemBioChem

Research Article
doi.org/10.1002/cbic.202300832

Chemistry Europe
European Chemical Societies Publishing

www.chembiochem.org

Amylose Dimerization in Solution Can Be Studied Using a Model System

Charlotte Nybro Dansholm,[a] Sebastian Meier,[a] and Sophie R. Beeren*[a]

Amylose, the linear polymer of α-1,4-linked glucopyranose units, is known to crystallize as a parallel double helix, but evidence of this duplex forming in solution has remained elusive for decades. We show how the dimerization of short amylose chains can be detected in solution using NMR spectroscopy when the glucans are labeled at the reducing-end with an aromatic moiety that overcomes chemical shift degeneracy leading to distinct signals for the single-stranded and duplex amylose. A set of α-1,4 glucans with varying lengths of 6, 12, 18, and 22 glucose units and a 4-aminobenzamide label were synthesized, enabling the first systematic thermodynamic study of the association of amylose in solution. The dimerization is enthalpically driven, entropically unfavorable and beyond a minimum length of 12, each additional pair of glucose residues stabilizes the duplex by 0.85 kJ mol^{-1}. This fundamental knowledge provides a basis for a quantitative understanding of starch structure, gelation and enzymatic digestion, and lays the foundations for the strategic use of α-1,4-glucans in the development of self-assembled materials.

Introduction

Glucose-based polysaccharides are the most abundant biomaterials in Nature. Their functions and physicochemical properties are directly linked to both the nature of their glycosidic linkages and the consequent possibilities for defined secondary structure and higher-order assemblies.[1] For example, in the solid state, α-1,4-glucans form left-handed double helices (amylose, Figure 1a),[2–4] β-1,4-glucans align in sheets (cellulose) and β-1,3-glucans form right-handed triple helices (curdlan).[1] α-1,4-glucans can also form single left-handed helices around hydrophobic guests (known as V-amylose), both in the solid state[5,6] and in aqueous solution:[7,8] a classic example is the binding of polyiodide to starch (Figure 1b).[9] The supramolecular organization of α-1,4-glucan chains in starch is critical for efficient energy storage in plants and impacts upon starch gelation and enzymatic digestion, which has wide-ranging implications in agriculture and food production.[10,11] The structure of starch has been the subject of extensive research over several decades, and yet the solution behavior of amylose has remained poorly understood. While it is well-established that amylose crystallizes in a parallel left-handed double helix,[2–4] evidence of this structure in solution has remained elusive.

The solid state double helical structure of amylose is found in two allomorphs: the closely packed A-amylose[2,3] and the more openly packed B-amylose.[4] Both consist of two left-handed parallel helices with six glucose units per turn (Figure 1a) and can be distinguished using solid-state ^{13}C NMR spectroscopy.[12] A minimum degree of polymerization (DP) of 10 is required for crystallization,[13] suggesting that almost two turns are needed to form a stable helix. Double helices within amylose gels have also been reported based on analysis by X-ray diffractometry,[14] ^{13}C CP/MAS NMR spectroscopy[15] and CryoTEM.[16]

Amylose in aqueous solution has been described as either a random coil, an extended coil, a random coil with extended helical segments or a wormlike helical conformation.[17,18] Cylindrical structures compatible with short double helices were detected during the enzymatic synthesis of amylose using SAXS.[19] Computational modelling of short amylose chains in solution suggests that the parallel double helix is the preferred conformation.[20]

Experimental investigation of the solution structure and dynamics of α-1,4-glucans is hampered by the severe NMR chemical shift degeneracy for homooligosaccharides in solution,[21] as well as the challenge of synthesizing or isolating individual oligosaccharides of specific length.[22] Seeberger and co-workers recently described the total synthesis of maltohexadecaose (**G16**) using automated glycan assembly.[23] Instead, we chose an enzymatic synthesis to obtain a mixture of α-1,4-glucans and successfully separated these chromatographically.[24,25] We synthesized a set of four different length labeled α-1,4-glucan oligosaccharides. Herein, we report our discovery that these short labeled amylose chains can dimerize in solution, allowing, for the first time, the quantification of the binding interaction between associating amylose chains in water.

[a] *Dr. C. Nybro Dansholm, Prof. Dr. S. Meier, Prof. Dr. S. R. Beeren*
Department of Chemistry
Technical University of Denmark
Kemitorvet Building 207, Kongens Lyngby, DK-2800, Denmark
E-mail: sopbee@kemi.dtu.dk

Supporting information for this article is available on the WWW under https://doi.org/10.1002/cbic.202300832

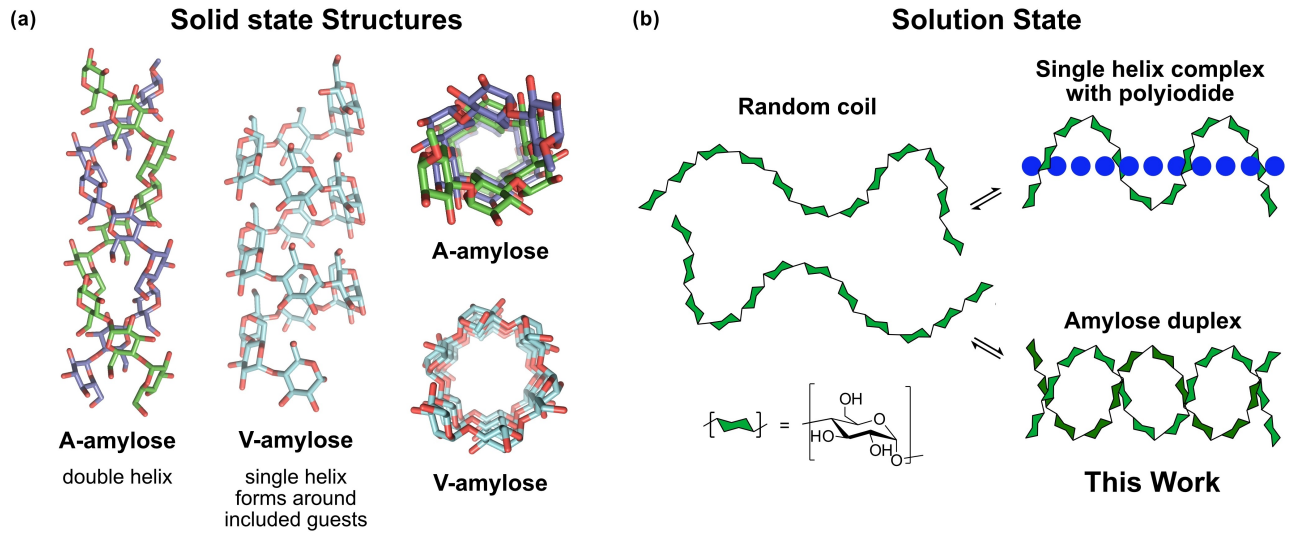

Figure 1. a) Double and single helical solid-state structures of amylose: A-amylose[3] and V-amylose with 1-butanol guest omitted.[6] b) Schematic illustration of the solution state structures of amylose: random coils can assembly into guest-included single helices or dimerize, as shown herein.

Results and Discussion

Four labeled maltooligosaccharides were synthesized with 6, 12, 18, and 22 glucopyranose units, and the fluorescent 2-aminobenzamide (**AB**) label attached at the reducing-end (hemiacetal) glucose (Scheme 1). Maltohexaose (**G6**) was first functionalized with 2-aminobenzamide (**AB**) via a reductive amination to obtain **G6-AB**. **G12-AB**, **G18-AB**, and **G22-AB** were then synthesized enzymatically by reaction of **G6-AB** (1 mM) with glucose-1-phosphate (15 mM) in the presence of glycogen phosphorylase (EC 2.4.1.1) (1 U/mL) in HEPES buffer (50 mM, pH 6.8) at 30 °C.[26,27] An excess of glucose-1-phosphate was employed to drive this reversible reaction towards elongation of the glucans. A mixture of different length α-1,4-glucans (**G3-AB**–**G30-AB**) was generated and preparative-scale HPLC with a hydrophilic interaction chromatography (HILIC) column enabled the isolation of **G12-AB**, **G18-AB**, and **G22-AB** on a mg-scale with very high purities (>99%, 98% and 96% by HPLC, respectively) (Figure 2).

Upon characterization of these isolated labeled maltooligosaccharides using NMR spectroscopy, we observed two sets of signals for **G12-AB**, **G18-AB** and **G22-AB** in aqueous solution

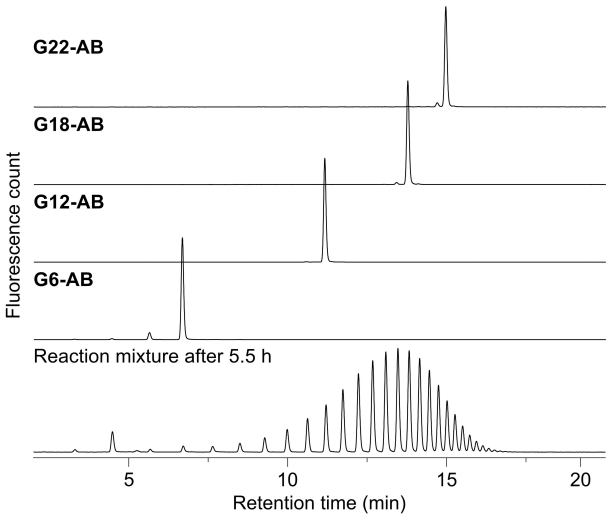

Figure 2. Four different length labeled α-1,4-glucans were isolated with high purity. Chromatograms (HPLC-FD, $I_{ex/em}$ = 356/436 nm) showing the isolated α-1–4-glucans and the product mixture prior to separation.

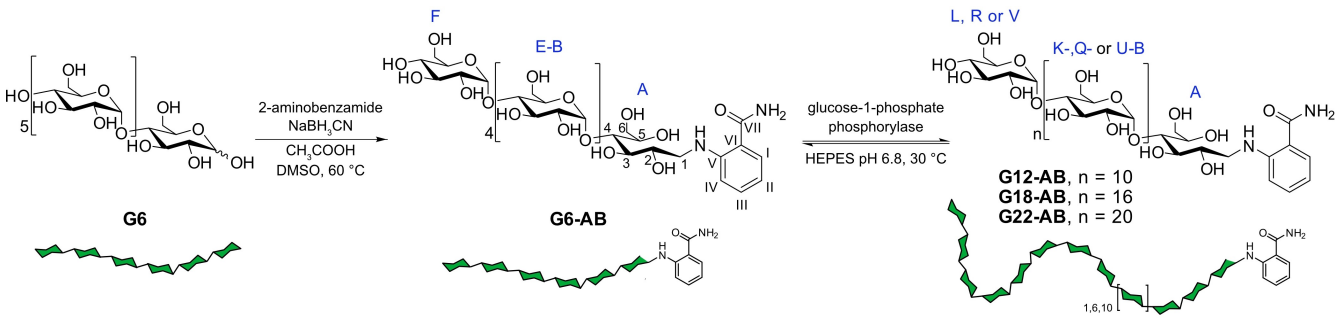

Scheme 1. Synthesis of a set of labeled α-1,4-glucans. Synthesis of AB-labeled maltohexaose (**G6-AB**) and the phosphorylase-catalyzed synthesis of α-1,4-glucans of different length (**G12-AB**, **G18-AB** and **G22-AB**).

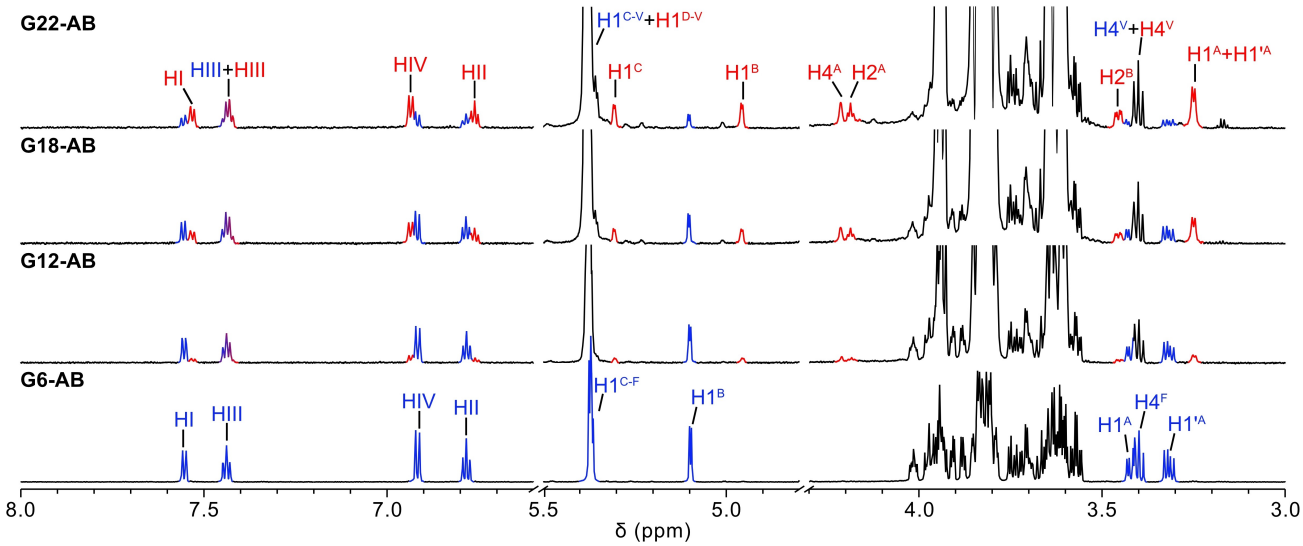

Figure 3. Dimerization of α-1,4-glucans was detected in solution for **G12-AB** and longer. ^{1}H NMR spectra of **G22-AB** (0.5 mM), **G18-AB** (0.5 mM), **G12-AB** (0.5 mM), and **G6-AB** (2.3 mM) in D_2O at 303 K. Discrete signals from single-stranded α-1,4-glucans and for the duplexes are coloured in blue and red, respectively.

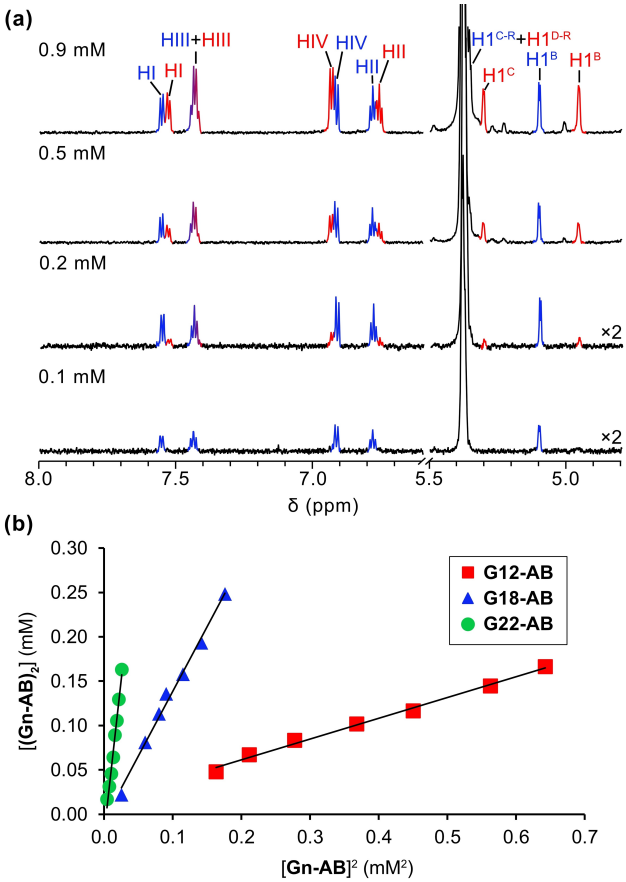

Figure 4. Dilution studies enabled determination of the dimerization constants for different length α-1,4-glucans. a) ^{1}H NMR spectra of **G18-AB** at different total concentrations in D_2O at 303 K. b) Plot of [(**Gn-AB**)$_2$] versus [**Gn-AB**]^2 at varying total concentrations used to determine the dimerization constants K_{dim}.

(Figure 3). Moreover, the relative intensity of the additional set of signals increased as the length of the glycan increased for samples at the same concentration.

We speculated that the second set of signals could result from dimerization, and thus performed dilution experiments. Figure 4a shows ^{1}H NMR spectra for the dilution series of **G18-AB** (see Figure S14 for full spectra). The ratio between the proposed duplex (signals highlighted in red) and monomer (signals highlighted in blue) decreased upon dilution and the duplex was not detectable at 0.1 mM. The duplex signals exhibited a larger linewidth indicating a larger molecular weight (Figure S12) and a DOSY experiment showed two distinct species (Figure S21). A slightly smaller diffusion coefficient was found for the proposed duplex, suggesting that it must have a compacted structure. Similar dilution experiments were performed for **G12-AB** and **G22-AB** and showed the same trend (Figures S12–S15).

A quantitative analysis of the NMR dilution study was necessary to distinguish dimerization from possible aggregation. By integration of the aromatic signal HI, at ~7.56 ppm for the monomer and at ~7.53 ppm for the proposed duplex, the concentrations of the duplex ([(**Gn-AB**)$_2$]) and monomer ([**Gn-AB**]) could be obtained, taking into consideration that [**Gn-AB**]$_T$ = [**Gn-AB**] + 2[**Gn-AB**]$_2$, where [**Gn-AB**]$_T$ is the total concentration of the oligosaccharide. In the case of dimerization, the equilibrium constant can be obtained from K_{dim} = [(**Gn-AB**)$_2$]/[**Gn-AB**]^2. Plots of [(**Gn-AB**)$_2$] versus [**Gn-AB**]^2 were made for **G12-AB**, **G18-AB** and **G22-AB** (Figure 4b). In each case, a linear correlation was observed, confirming that the additional set of signals in the NMR spectra were due to dimerization. From the gradients, dimerization constants (K_{dim}) of 230 M^{-1}, 1500 M^{-1}

and 7000 M^{-1} were obtained for **G12-AB**, **G18-AB** and **G22-AB**, respectively (Table 1).

A plot of △G° against degree of polymerization (DP revealed a linear relationship between the length of the α-1,4-glucan and the Gibbs free energy change upon dimerization (△G° = −0.85×DP−3.5 kJmol^{-1}) (Figure 5a). From the gradient we could compute that each additional pair of glucose residues stabilizes the duplex by 0.85 kJmol^{-1}. Extrapolating backwards to shorter α-1,4-glucans, an association constant of 29 M^{-1} would be predicted for **G6-AB**. However, dimerization of **G6-AB** was not observed even at 29 mM, at which concentration 6.8 mM duplex and 15.2 mM monomer would be predicted if the linear trend continued (Figure S16). It must therefore be inferred that, as seen in the solid state,[13] there is a minimum length requirement for the formation of amylose duplexes in solution, and, in the case of these labeled α-1,4-glucans, that minimum length occurs between DP6 and DP12.

To obtain thermodynamic parameters for the dimerization process, ^{1}H NMR spectra were recorded for **G12-AB**, **G18-AB** and **G22-AB** at different temperatures (303–333 K) (Figure S17–S20), and a van't Hoff analysis was made (Figure 5b). The dependence of △G°, △H° and △S° on the length of the α-1,4-glucans is shown in Figure 5a and Table 1. Duplex formation in solution is enthalpically favourable and entropically unfavourable. In the solid state, the amylose double helix is stabilized by an extensive intermolecular hydrogen-bonding network.[2–4] The formation of such a network of intermolecular hydrogen bonds could provide an enthalpic benefit also in solution, whereas an entropic penalty would be expected based on a loss of conformational flexibility and translational freedom upon dimerization. The observed thermodynamic signature could also indicate that a non-classical hydrophobic effect is driving the dimerization process, although this phenomenon is more typically associated with complexation within macrocycles.[28] Duplex formation is increasingly enthalpically favourable and

Table 1. Binding parameters for the dimerization of the linear α-1,4-glucans.

	K_{dim} (M^{-1})[a]	△G° (kJ mol^{-1})	△H° (kJ mol^{-1})	T△S° (kJ mol^{-1})
G12-AB	(2.3 ± 0.8)×10^2	−13.7 ± 0.1	−16.9 ± 4.3	−2.4 ± 4.1
G18-AB	(1.5 ± 0.6)×10^3	−18.4 ± 0.1	−24.4 ± 4.0	−5.3 ± 3.8
G22-AB	(7.0 ± 0.3)×10^3	−22.3 ± 0.1	−28.5 ± 5.3	−6.0 ± 5.3

[a] Determined in D_2O at 303 K.

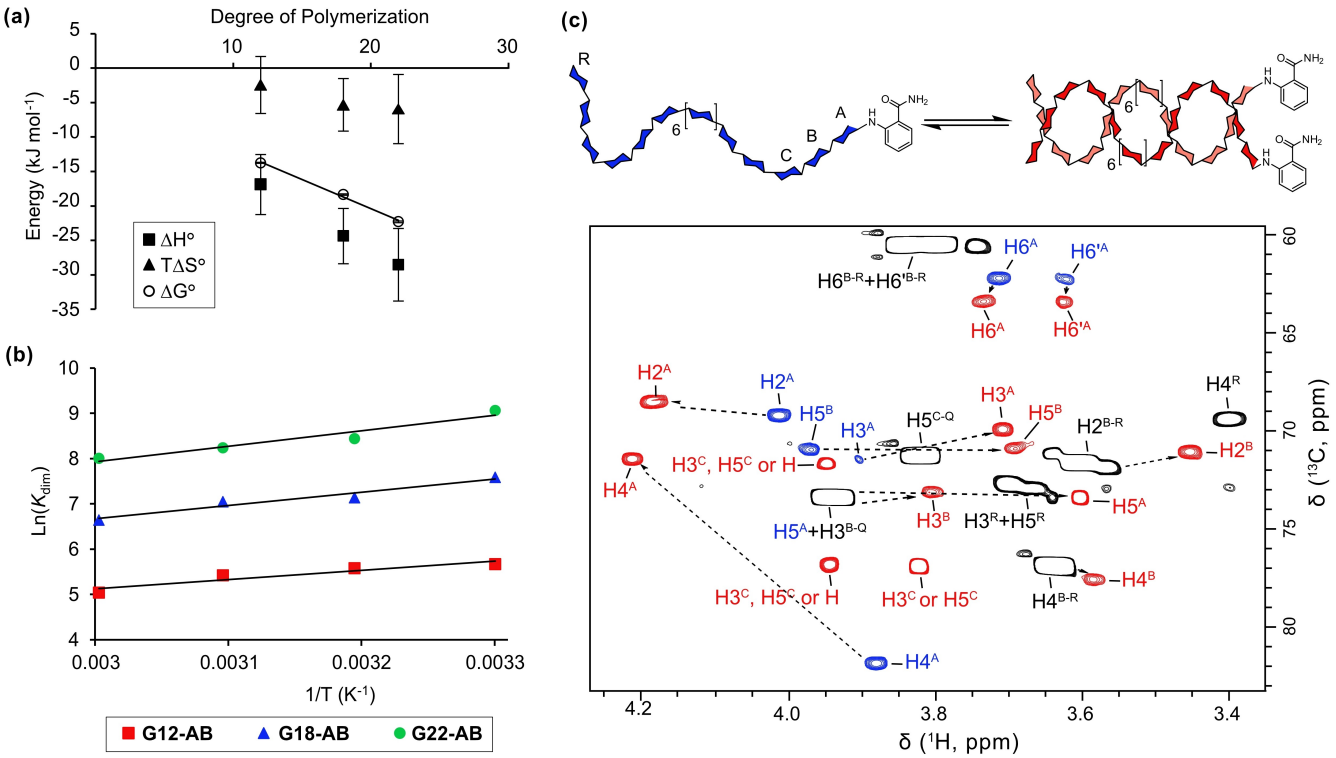

Figure 5. Dimerization in enthalpically driven, linearly dependent on the glycan length and occurs with the glycans oriented parallel. a) Plot of △G°, △H° and T△S° for the dimerization as a function of the degree of polymerization (DP) of the α-1,4-glucans. b) Van 't Hoff plot for the dimerization of the linear α-1,4-glucans at 303–333 K. c) Partial ^{1}H–^{13}C HSQC NMR spectrum of **G18-AB** (0.9 mM) in D_2O at 303 K. The signals corresponding to the monomer and the duplex are shown in blue and red, respectively, whereas overlapping signals are shown in black.

increasingly entropically unfavourable as the length of the α-1,4-glucan increases. However, the entropic cost per glucose unit decreases as the glucan length increases, and thus duplex formation in solution is increasingly favourable as the α-1,4-glucan length increases.

It was expected that the aminobenzamide (**AB**) label could play a role in stabilizing the duplexes. To investigate this, we obtained a commercial sample of unlabeled maltoundecaose (**G11**). The NMR spectrum of **G11** showed only a single set of signals, and the spectrum was unchanged upon dilution and temperature variation (Figures S22 and S23). On the other hand, ITC experiments did indicate that an endothermic dissociation process took place upon dilution of **G11** but not **G6** (Figures S24 and S25). Evidently, the **AB** label plays a key role in overcoming the chemical shift degeneracy in the NMR spectra of these α-1,4-glucans such that signals from the monomer and the duplex become distinct from one another. It is also likely that the **AB** label contributes to the stabilization of these duplexes, but as **G6-AB** does not dimerize even at high concentration, the stabilizing influence of the **AB** label must be weak, and a specific interaction between the oligosaccharide chains of sufficient length is required for duplex formation. The 'per glucose' stabilization energy of 0.85 $kJmol^{-1}$, calculated for glucans of at least DP12 (Figure 5a), is independent of the **AB** label, and can, thus, be used to predict the self-association of native amylose, and shorter α-1,4-glucans, in solution.

In the solid state, the amylose double helix is left-handed and parallel.[2–4] Structural assignment of the duplex in solution suggests that this arrangement is maintained in solution, at least, for these model compounds. A full assignment of signals in the ^{1}H–^{13}C HSQC spectra (Figures S6–S11) of the monomer/duplex mixtures for **G12-AB**, **G18-AB** and **G22-AB** was performed (Tables S4–S6). The partial ^{1}H–^{13}C HSQC spectrum of **G18-AB** is shown in Figure 5c, wherein distinct signals from the monomer are colored blue, distinct signals from the duplex are colored red, and signals where the monomer and duplex overlap are colored in black. For the protons on the sugar residues A and B, which are closest to the AB label (signals $H1^{A}$–$H6^{A}$ and $H1^{B}$–$H5^{B}$), two distinct sets of signals are observed for the monomer and duplex, while the signals for the protons on the non-reducing end glucose ($H1^{R}$–$H6^{R}$) are completely overlapped. This suggests that the two oligosaccharides in the duplex are parallel. In an antiparallel orientation, a change in the chemical shift for the protons at the non-reducing end would be expected upon duplex formation, as this would bring the non-reducing end glucose unit near the aromatic AB-label and some effect of the aromatic ring current would be expected. The same observations were made for **G12-AB** and **G22-AB**, and these experimental results are consistent with reported solution state simulations suggesting that parallel duplex formation is favored.[20]

Conclusions

In conclusion, we have identified a model system whereby the dimerization of short amylose chains can be observed and studied in solution. By installation of a 2-aminobenzamide label at the reducing-end of a set of α-1,4-glucans, the dimerization could be visualized using NMR spectroscopy. Quantitative information on polysaccharide interactions is generally very difficult to obtain and therefore often considered only as average or global values. While model peptides have been extensively used to help understand the thermodynamics and structural basis for folding in proteins,[29–31] the use of model oligosaccharides to explore the conformation and assembly of polysaccharides has, until recently, been very limited.[22,32] The synthesis and isolation of this set of individual α-1,4-glucans of different lengths (DP 6, 12, 18, and 22) as model compounds has allowed for a systematic study and quantification of the 'per glucose' interactions between chains of this important biopolymer. Specifically, the dimerization of amylose is enthalpically driven, entropically unfavourable, and beyond a length of 12 glucose units there is a linear correlation between the stability of the duplex and the α-1,4-glucan length: each additional pair of glucose residues stabilizes the duplex by 0.85 $kJ\,mol^{-1}$. This fundamental knowledge is critical to understanding the physicochemical properties, structure, biosynthesis and enzymatic digestion of starch, and can provide a quantitative basis for the design and self-assembly of α-1,4-glucan-based materials.

Supporting Information

The authors have cited additional references within the Supporting Information.[33]

Acknowledgements

We are grateful to the Villum Foundation (Grant number 15482), Novo Nordisk Foundation (NNF19OC0057672) and the European Research Council (ERC-Starting Grant ENZYME-DCC) for financial support. High-field NMR spectra were acquired at the NMR Center DTU funded by the Villum Foundation. We thank Prof. M. Pittelkow, Prof. B. Svensson and Prof. M. A. Hachem for use of their ITC instruments, Dr. M. Madsen for help with ITC measurements and the Carlsberg Foundation for funding of ITC equipment to M. A. Hachem.

Conflict of Interests

The authors declare no conflict of interest.

Data Availability Statement

The data that support the findings of this study are available in the supplementary material of this article.

Keywords: supramolecular chemistry · carbohydrates · NMR spectroscopy · amylose · helices

[1] G. Fittolani, P. H. Seeberger, M. Delbianco, *Pept. Sci.* **2020**, *112*, 24124.
[2] A. Imberty, H. Chanzy, S. Pérez, A. Buléon, V. Tran, *J. Mol. Biol.* **1988**, *201*, 365.
[3] D. Popov, A. Buléon, M. Burghammer, H. Chanzy, N. Montesanti, J. L. Putaux, G. Potocki-Véronese, C. Riekel, *Macromolecules* **2009**, *42*, 1167.
[4] A. Imberty, S. Perez, *Biopolymers* **1988**, *27*, 1205.
[5] K. Takeo, A. Tokumura, T. Kuge, *Starch/Staerke* **1973**, *25*, 357.
[6] C. A. K. Le, Y. Ogawa, F. Dubreuil, F. Grimaud, K. Mazeau, G. R. Ziegler, S. Tanwar, Y. Nishiyama, G. Potocki-Veronese, L. Choisnard, D. Wouessidjewe, J. L. Putaux, *Carbohydr. Polym.* **2021**, *261*, 117885.
[7] J. A. Putseys, L. Lamberts, J. A. Delcour, *J. Cereal Sci.* **2010**, *51*, 238.
[8] S. Meier, S. R. Beeren, *J. Am. Chem. Soc.* **2014**, *136*, 11284.
[9] R. E. Rundle, D. French, *J. Am. Chem. Soc.* **1943**, *65*, 1707.
[10] S. Pérez, E. Bertoft, *Starch/Staerke* **2010**, *62*, 389.
[11] A. Damager, S. B. Engelsen, A. Blennow, B. Lindberg Møller, M. S. Motawia, *Chem. Rev.* **2010**, *110*, 2049.
[12] M. J. Gidley, S. M. Bociek, *J. Am. Chem. Soc.* **1988**, *110*, 3820.
[13] M. J. Gidley, P. V. Bulpin, *Carbohydr. Res.* **1987**, *161*, 291.
[14] V. M. Leloup, P. Colonna, S. G. Ring, K. Roberts, B. Wells, *Carbohydr. Polym.* **1992**, *18*, 189.
[15] M. J. Gidley, *Macromolecules* **1989**, *22*, 351.
[16] J.-L. Putaux, A. Buléon, H. Chanzy, *Macromolecules* **2000**, *33*, 6416.
[17] N. W. H. Cheetham, L. Tao, *Carbohydr. Polym.* **1998**, *35*, 287.
[18] E. Bertoft, *Agronomy* **2017**, *7*, 56.
[19] P. Roblin, G. Potocki-Véronèse, D. Guieysse, F. Guerin, M. A. V. Axelos, J. Perez, A. Buléon, *Biomacromolecules* **2013**, *14*, 232.
[20] B. M. Sattelle, A. Almond, *Phys. Chem. Chem. Phys.* **2014**, *16*, 8119.
[21] S. R. Beeren, S. Meier, *Chem. Commun.* **2015**, *51*, 3073.
[22] M. Delbianco, A. Kononov, A. Poveda, A. Yu, T. Diercks, J. Jiménez-Barbero, P. H. Seeberger, *J. Am. Chem. Soc.* **2018**, *140*, 5421.
[23] Y. Zhu, M. Delbianco, M. H. Seeberger, *J. Am. Chem. Soc.* **2021**, *143*, 9758.
[24] P. J. Smith, M. E. Ortiz-Soto, C. Roth, W. J. Barnes, J. Seibel, B. R. Urbanowicz, F. Pfrengle, *ACS Sustainable Chem. Eng.* **2020**, *8*, 11853.
[25] J.-I. Kadokawa, *Chem. Rev.* **2011**, *111*, 4308.
[26] J.-I. Kadokawa, *Methods Enzymol.* **2019**, *627*, 189.
[27] E. C. O'Neill, R. A. Field, *Carbohydr. Res.* **2015**, *403*, 23.
[28] F. Biedermann, W. M. Nau, H.-J. Schneider, *Angew. Chem. Int. Ed.* **2014**, *53*, 11158.
[29] N. V. Ilawe, A. R. Raeber, R. Schweitzer-Stenner, S. E. Toal, B. M. Wong, *Phys. Chem. Chem. Phys.* **2015**, *17*, 24917.
[30] R. Schweitzer-Stenner, *Phys. Chem. Chem. Phys.* **2023**, *25*, 11908.
[31] J. Venkatraman, S. C. Shankaramma, P. Balaram, *Chem. Rev.* **2001**, *101*, 3131.
[32] N. Hribernik, D. Vargová, M. C. S. Dal Colle, J. H. Lim, G. Fittolani, Y. Yu, J. Fujihara, K. Ludwig, P. H. Seeberger, Y. Ogawa, M. Delbianco, *Angew. Chem. Int. Ed.* **2023**, *62*, e202310357.
[33] S. A. Cooke, S. Ó Jónsdóttir, P. Westh, *J. Chem. Eng. Data* **2002**, *47*, 1185.

Manuscript received: December 8, 2023
Revised manuscript received: January 5, 2024
Accepted manuscript online: January 14, 2024
Version of record online: February 8, 2024